SPECTRAL ANALYSIS OF ASTER AND HYPERION DATA FOR GEOLOGICAL CLASSIFICATION OF VOLCANO TEIDE

Alessandro Piscini,[1] Stefania Amici,[1] and David Pieri[2]

[1]Istituto Nazionale di Geofisica e Vulcanologia, Rome, Italy
[2] Jet Propulsion Laboratory, Pasadena, California USA

ABSTRACT

This work is an evaluation to which degree geological information can be obtained from modern remote sensing systems like the multispectral ASTER or the hyperspectral Hyperion sensor for a volcanic region like Teide Volcano (Tenerife, Canary Islands). To account for the enhanced information content these sensors provide, hyperspectral analysis methods, incorporating for example Minimum Noise Fraction-Transformation (MNF) for data quality assessment and noise reduction as well as Spectral Angle Mapper (SAM) and Support Vector Machine (SVM) for supervised classification, were applied. Ground Truth reflectance data were obtained with a FieldSpec Pro measurements campaign conducted during later summer of 2007 in the frame of the EC project PREVIEW (http://www.preview-risk.com/).

Index Terms— Teide, classification, hyperspectral sensors, ASTER, Hyperion, reflectance spectra

1. INTRODUCTION

The Canarian Archipelago is made up of seven islands that represent different stages of geologic evolution [1], [3], [4], [5], [6]. Tenerife Island is the central Island of the archipelago and his Volcano Teide (Pico del Teide) is a predominate feature.

The Pico del Teide structure is the exposed part of a giant volcanic construct that extends from the floor of the eastern central Atlantic with peaks ranging from 2370 m to 3718 m at the summit of Teide volcano. The subaerial history of the island began in the late Miocene Plio-Quaternary and post-shield volcanism on Tenerife and has been characterized by the cyclic development of petrologically evolved eruptive centers. The most recent eruptive cycle has produced the twin strato-volcanoes Pico del Teide (PT) and Pico Viejo (PV), and numerous flank-vent systems, whose products collectively form the PT/PV formation. Like previous cycles, PT/PV volcanism has involved central activity and persistent eruptions from prominent rifts recent geological investigations of Teide have focused on the Pliocene-Holocene late stage eruptive activity.

Mapping of exposed flow units and reconstruction of eruption sequences was carried out by Carracedo et al. [1], [4], [5]. Recent eruptive activity on Tenerife (e.g., 200 ka to present) has also been described and characterized by them [7]. Until now, however, no spectroscopic characterization of the Teide volcanic has been available. In 2007, however, a remote sensing data validation campaign, funded by the European Community under the PREVIEW FP6 project was carried out, accomplishing multiple aims.

During the campaign, field Reflectance and Emissivity spectra were acquired representing a ground truth library for scientific investigation (i.e. for validation of satellite data, and a training basis for supervised classification). On demand acquisition of Hyperion and ASTER data were attempted, however, weather conditions were not acceptable during satellite overpasses (e.g., 80% cloud cover) and so we have used archived data for this study.

2. METHODS

2.1 Data pre-processing

The multispectral Advanced Spaceborne Thermal Emission and reflection Radiometer (ASTER) was launched on 19 December 1999 on board NASA's Terra satellite. It has three bands in the VNIR (15 m spatial resolution) and six bands in the SWIR (30 m spatial resolution) wavelength region [10]. In particular, the SWIR bands were intended for the discrimination of minerals or rock types. For spectral analyses reported here, an AST_07 Surface Reflectance product covering the study area was utilized, having been acquired on August 4, 2007 [2], only 30 days before the campaign.

The Hyperion sensor, onboard NASA's EO-1 platform, is a pioneering spaceborne imaging spectrometer covering the wavelength region from 0.4 to 2.5 μm with 220 bands at 10 nm spectral resolution and 30 m spatial resolution. For the current study, L1R-Data ('At-Sensor Radiance') from November 13, 2003 was used.

The preprocessing of the ASTER data consisted of resampling VNIR bands to 30 m spatial resolution, and the combination of the VNIR and SWIR data into a 9-band imagecube. Regarding the Hyperion data preprocessing, due to signal-to-noise issues and other radiometric difficulties, only 198 bands are calibrated in this data product (for further details see [14]). As a result, a subset of 196 bands, were appropriate for further analysis. As with ASTER data, we applied a scaling factor to convert the dataset in radiometric units. The image was geo-referenced using ground control points (GCPs) to re-project the ASTER image. Surface reflectance was retrieved using the Fast Line-of-sight Atmospheric Analysis of Spectral Hypercubes (FLAASH) [8] algorithm from the commercial ENVI® software package. In order to reduce noise in the Hyperion image and improve classification results, a Minimum Noise Fraction-Image (MNF) was generated for data dimensionality estimation and reduction, thereby decorrelating useful information and separating noise [11]. A statistics based Lee filter [13] was then applied to the inverse MNF Hyperion image.

2.2 Classification methods

Image classification is a processing technique in which quantitative classification decisions are made on the basis of the data present in the image, grouping pixels or regions of the image into classes (e.g., representing different ground–cover or spectrally distinct terrane types).

Classification techniques can be broadly divided into two types: supervised classification and unsupervised classification. In supervised classification, information about the distribution of spectral unit types in part or parts of the image is used to initiate the process. Pixels or groups of pixels corresponding to known spectral types are called training data or training areas and are used to 'train' the classification process to recognise other, similar pixels.

In this work we applied two ENVI® supervised classification methods, Spectral Angle Mapper (SAM) and Support Vector Machine (SVM). SAM is a physically based classification algorithm that compares the spectral similarity between surface reflectance image spectra and reference spectra, treating them as vectors in a space with the dimensionality equal to the number of bands [12]. Image spectra are assigned to the reference spectrum class that yields the smallest calculated angle. The SVM classifier is derived from statistical learning theory. It separates classes with a decision surface that maximizes the margin between the classes [9]. The training suite (18 classes) was selected by using both "ground truth" acquired during field campaign, and visual selection. The ground true classes are a suite of 8 reflectance spectra (Fig.1) in the range 0.35-2.5 µm acquired by a portable FieldSpec spectrometer.

The spectra have been chosen according to the following criteria: 1) to be as high as possible, wide, plane and open areas of homogenous surface material; 2) to be easy reachable on the field and to recognizable and localizable on the image; 3) they have to be located in a well know geological setting; 4) they have to be in the field of view of both ASTER and Hyperion images. The remaining

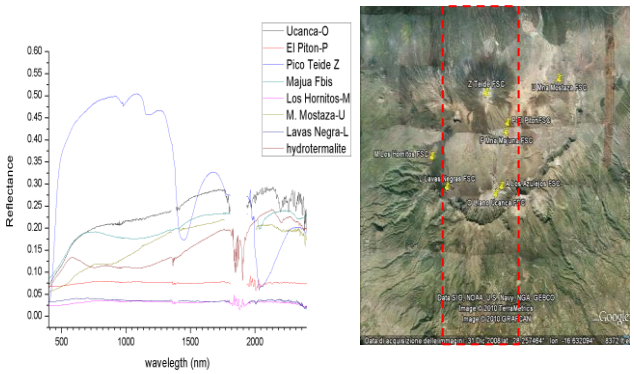

Figure1 Ground true reflectance spectra acquired by FieldSpec (left). The position of the points are located on Google Earth by their latitude and longitude.

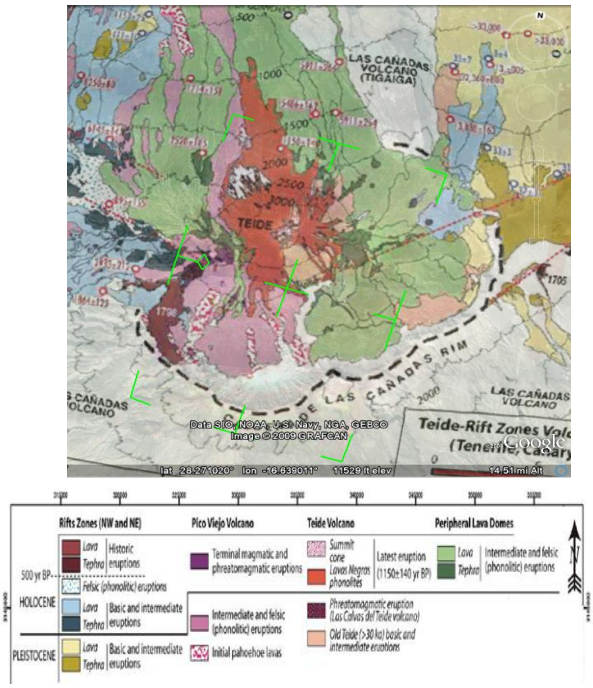

Figure 2. Geological map of Volcano Teide, Tenerife [7].

10 spectra have been chosen by visual inspection referring to geological map. Training datasets for classification was selected in this way: starting from ground true measurements first we generate the 18 classes and by populating them by using a growing sampling algorithm. Classes so obtained were sub sampled by using a stratified random sampling method.

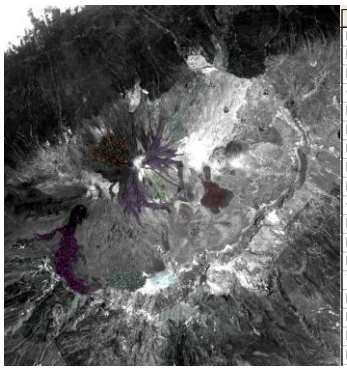

ROI Name	Color	Pixels
Mna Majua - F	Red	4
Mna Majua - F bis	Red3	15
El Piton - P	Blue	8
v. de la Candela	Yellow	9
Llano de Ucanca - O	Cyan	71
Lava del Chaorra - L	Magenta	397
Boca Tauce - S	Maroon	13
Lavas negras sud	Purple	396
Lavas negras nord	Coral	270
veg	Sea Green	1,391
Mna Chafari sud	Aquamarine	166
Mancha Ruana	Orchid	27
la Orotava	Sienna	6
Teide Phase Final	Chartreuse	57
Pico Teide - Z	Red1	1
Mauja bis	Red2	141
De Cruz de Tea	Thistle	97
Mna Blanca	Green	3

Figure 3. Ground Truth Class Training set (left) and description table (right) for ASTER.

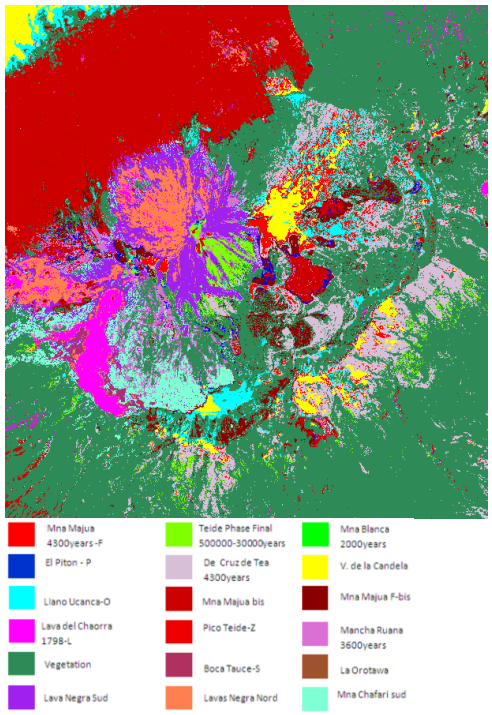

Figure 4 ASTER SVM classification map and class descriptions.

	Prod. Acc. (Percent)	
Class	ASTER	Hyperion
Mna Majua - F	92.5	50.74
Mna Majua - F bis	48.03	65.13
El Piton - P	2.6	49.67
v. de la Cand	96.7	84.5
Llano de Ucan	97.88	95.53
Lava del Chao	96.12	79.31
Boca Tauce -	45.86	0
Lavas negras S	96.27	79.36
Lavas negras N	94.67	88.79
veg	99.49	89.57
Mna Chafari s	95.85	96.98
Mancha Ruana	93.66	48.81
la Orotava	40	0
Teide Phase F	96.13	91.85
Pico Teide -	100	0
Mauja bis	99.08	97.81
De Cruz de Te	97.23	87.47
Mna Blanca	0	84.02

Table 1. Producer Accuracy for ASTER and Hyperion SVM classification.

3. RESULTS DISCUSSION

SAM and SVM classifications accuracies were estimated calculating the confusion matrices. An overall accuracy of 66.2716% and a K coefficient of 0.6052 for ASTER, and an overall accuracy of 59.4693% and a K coefficient of 0.5613 for EO1-Hyperion were achieved with SAM classification. Best results were obtained with SVM classification on both images: an overall accuracy of 96.8284% and K coefficient of 0.9574 for ASTER and an overall accuracy of 85.7787% and a K coefficient of 0.84 for EO1-Hyperion were achieved. When considering the Producer Accuracy for each class, we noticed that it is more than 90% for ASTER, except for classes as indicated in Table 1. Instead, Hyperion classification has lower Producer Accuracy values and doesn't improve results, with the exception of classes El Piton and Mna Majua F Bis. Furthemore, three classes—Boca Tauce, La Orotava and Pico Teide—have not been classified.

The classification maps for ASTER and Hyperion, obtained by using the SVM method, represented in Figures 4 and 5 respectively, have been compared to geological map of Volcano Teide (Fig. 2) [7]. They clearly demonstrate good correspondence among the classes and the geological units.

4. CONCLUSIONS

We report here the first spectral characterization of Volcano Teide carried out using combined in situ field and satellite hyperspectral and multispectral data. The central part of Teide was classified utilizing the both SAM and SVM supervised methods within the ENVI® software package. Comparisons between the classification image obtained by using the SVM method with both Hyperion and ASTER data and the Teide geological map show good formal statistical correspondence between the classes and the geological units. Also a good qualitative visual correspondence between the classes and the geological units is evident. On inspection, the ASTER classification map shows a wider presence of vegetation as contrasted with the Hyperion map. This difference may be due to a seasonal effect (i.e., Hyperion data were acquired in November, ASTER in August), or the three-year time difference may have allowed additional vegetation growth (i.e., Hyperion in 2003 vs. ASTER in 2007). The multispectral character of ASTER data versus the hyperspectral character of Hyperion data may have contributed to this difference, as well, although we think this effect is probably minimal. Overall the classification results obtained from Hyperion and ASTER data appear promising and confirm the utility of both as effective tools for volcanological mapping.

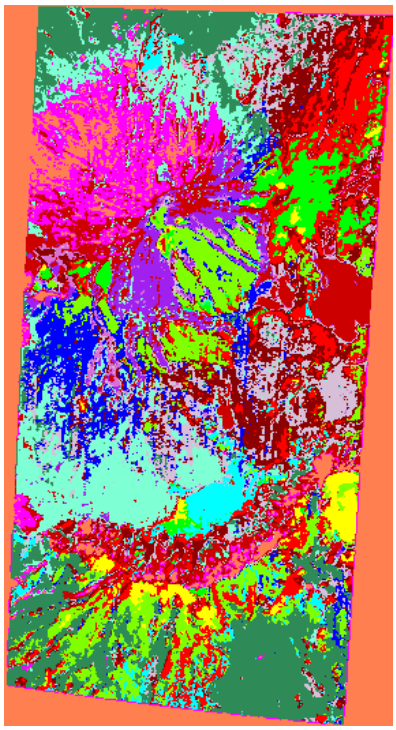

Figure 5. EO1-Hyperion SVM classification map. Classes are described in fig 4.

5. AKNOWLEDGEMENT

We would like to thank the INGV-Teide campaign field team: M.F. Buongiorno, M. Musacchio, V. Lombardo, S. Corradini, Dr. M.I. Pannaccione Apa. We express our acknowledgements to Director of "Planificación y Operaciones de Emergencias" Dr. Fernando Clavijo Redondo, and Dr. Sergio Barrera Rodriguez, Dirección General de Seguridad y Emergencias, Gobierno de Canarias, that made possible our fieldwork campaign all along the Natural Park of Teide volcano in Tenerife Island. We thank the European Community, which provided funds for the Preview project, and we thank the NASA ASTER and Hyperion spacecraft teams for the data acquisitions and processing. This work was carried out, in part, under contract to the NASA Earth Surface and Interiors Program at the Jet Propulsion Laboratory of the California Institute of Technology.

6. REFERENCES

[1] G.J., Ablay, and J. Martí, "Stratigraphy, structure, and volcanic evolution of the Pico Teide–Pico Viejo formation, Tenerife, Canary Islands" Journal of Volcanology and Geothermal Research, v. 103, p. 175–208, doi: 10.1016/S0377-0273(00)00224-9, 2000.

[2] M. Abrams, "The Advanced Thermal Emission and Reflection Radiometer (ASTER): data products for the high spatial resolution imager on NASA's Terra platform", International Journal of Remote Sensing, 21(5), pp. 847-859, 2000.

[3] J.C. Carracedo, S. Day, H. Guillou, E. Rodríguez Badiola, J.A. Canas, and , F.J. Pérez Torrado, " Hotspot volcanism close to a passive continental margin: The Canary Islands", Geological Magazine, v. 135, p. 591– 604, doi: 10.1017/S0016756898001447, 1998.

[4] J.C Carracedo," Growth, structure, instability and collapse of Canarian volcanoes and comparisons with Hawaiian volcanoes: Journal of Volcanology and Geothermal", Research Special Issue, v. 94, p. 1–19, 1999.

[5] J.C. Carracedo E. Rodríguez Badiola, H. Guillou, J. De La Nuez, and F.J. Pérez Torrado, Geology and volcanology of La Palma and El Hierro (Canary Islands): Estudios Geológicos, v. 57, p. 175–273, 2001.

[6] J.C. Carracedo, F.J. Pérez Torrado, E. Ancochea, J. Meco, F. Hernán, C.R. Cubas, R. Casillas, E. Rodríguez Badiola, and A. Ahijado, Cenozoic volcanism II: The Canary Islands, in Gibbons, W., and Moreno, T., eds., The geology of Spain: London, Geological Society [London], 632 p, 2002.

[7] J.C. Carracedo, E. Rodríguez Badio, H. Guillou, M. Paterne, S. F.J. Scaillet, R. Pérez Torrado Paris, U. Fra-Paleo, A. Hansen, "Eruptive and structural history of Teide Volcano and rift zones of Tenerife", Canary Islands GSA Bulletin; September/October 2007; v. 119; no. 9/10; p. 1027–1051; doi: 10.1130/B26087.1; 13 fi gures; 3 tables; Data Repository item 2007144, 2007.

[8] EO-1 User Guide 2003, USGS Earth Resources Observation System Data Centre (EDC), 2003.

[9] G.M. Foody and A. Mathur, "A Relative Evaluation of Multiclass Image classification by Support Vector Machines," IEEE Trans. Geoscience Remote Sens., vol. 42, pp. 1335-1343, 2004.

[10] H. Fujisada, "Design and performance of ASTER instrument, Proceedings of SPIE", 2583, pp. 16-25, 1995.

[11] Green, A.A., Berman, M., Switzer, P. & Craig, M.D., 1988. A Transformation for Ordering Multispectral Data in Terms of Image Quality with Implications for Noise Removal. IEEE Transactions on Geoscience and Remote Sensing, 26(1), pp. 65-74.

[12] J.R. Jenson, Introductory Digital Image Processing. A Remote Sensing Perspective. Pearson, Prentice Hall, Upper Saddle River, 2005.

[13]Lee, Jong-Sen, "Digital Image Enhancement and Noise Filtering by Use of Local Statistics," IEEE Transactions on Pattern Analysis and Machine Intelligence, Vol PAMI-2, No.2, March 1980, pp. 165-168.

[14] J.S. Pearlman, P.S. Barry, C.C Segal, J. Shepanski, D. Beiso, & S.L. Carman, "Hyperion, a Space-Based Imaging Spectrometer", IEEE Transactions on Geoscience and Remote Sensing, 41(6), pp. 1160-1173, 2003.